Electronic Supporting Information

Photocatalytic hydrogen production from water in self-assembled supramolecular iridium-cobalt systems

Sk. Jasimuddin,[a] Kazunori Fukuju,[a] Joe Otsuki [a] and Ken Sakai[b]

[a] *College of Science and Technology, Nihon University, 1-8-14 Kanda Surugadai, Chiyoda-ku, Tokyo 101-8308, Japan*

[b] *Department of Chemistry, Faculty of Science, Kyushu University, Hakozaki 6-10-1. Higashi-ku, Fukuoka, 812-8581, Japan*

Experimental

General experimental information. Solvents and reagents were of reagent grade and used without further purification. $[Ir(ppy)_2Cl]_2$,[1] $[Ir(ppy)_2(bpy)](PF_6)$,[2] $[Co(bpy)_3](PF_6)_2$,[3] 1,2-bis[4-(4'-methyl-2,2'-bipyridyl)]ethane (L1),[4] 1,3-bis(4'-methyl-2,2'-bipyridyl-4-yl)-2-propanol (L2),[5] 1,2-bis[5-(5'-methyl-2,2'-bipyridyl)]ethane (L3)[4a,5] and bis(2,2'-bipyridin-5-yl)ethyne (L4)[6] were synthesised and purified according to the reported procedures. ^{1}H-NMR spectra were recorded on a JEOL JNM-ECX400 spectrometer. ESI-HR mass spectra were obtained with an Agilent 1100LC/MSD mass spectrometer. Uv-vis and luminescence data were obtained using Shimadzu UV-2400PC and RF 5300PC spectrophotometer, respectively. Emission decays in the nanosecond time regime were recorded on an Iwatsu DS-4262 digitizing oscilloscope equipped with a Hamamatsu R928 photomultiplier tube. The excitation source was a N_2 laser (337 nm, Usho KEN-1520). The grating monochromator used was a Jobin Vyvon H-20 instrument. Data acquisitions were carried out up to 1024 scans. In all the measurements, each sample solution was purged with Ar for at least 15 minutes before the measurement. Electrochemical measurements were carried out with a Hokuto Denko HZ-3000 voltammetric analyzer. The electrochemical cell, maintained under Ar, was equipped with a Pt disk working electrode, a Pt wire counter electrode, and an Ag wire as a pseudo reference electrode. The supporting electrolyte solution was 0.01 M Bu_4NPF_6 in CH_3CN. The scan rate was 100 mV/s. Potentials were reported with respect to the internal Fc^+/Fc couple.

$[Ir\text{-}X]^+$ (X = L1–L4). Synthesis of $[Ir\text{-}X]^+$ is exemplified by that of $[Ir\text{-}L1]^+$. The dimeric Ir(III) complex $[Ir(ppy)_2Cl]_2$ (0.035 g, 0.03 mmol) was dissolved in CH_2Cl_2 (5 mL) under Ar.

To this solution, L1 (0.034 g, 0.09 mmol) was added. The reaction mixture was refluxed under Ar for 4 h. The solvent was evaporated and the resulting solid was purified by column chromatography on Sephadex LH-20 (eluent CH_3CN). The second yellow band was collected to give the desired product (0.027 g, 47%).

[Ir-L1]$^+$. ^{1}H-NMR ($CDCl_3$): δ 9.93 (1H, s), 9.79 (1H, s), 8.53 (1H, d, *J* = 5.0 Hz), 8.49 (1H, d, *J* = 4.6 Hz), 8.2–8.3 (2H, m), 7.89 (2H, d, *J* = 7.8 Hz), 7.73 (2H, m), 7.67 (4H, m), 7.50 (1H, m), 7.41 (1H, m), 7.3–7.2 (2H, overlapped with $CHCl_3$), 7.13 (2H, d, *J* = 5.5 Hz), 7.1–6.85 (6H, m), 6.28 (2H, t, *J* = 6.9 Hz), 3.37 (4H, m, CH_2CH_2), 2.70 (3H, s, CH_3), 2.44 (3H, s, CH_3); ESI–HRMS (CH_3CN): *m*/*z* calcd. for $C_{46}H_{38}IrN_6^+$ ([M–Cl]$^+$), 867.2782; found, 867.2889.

[Ir-L2]$^+$. ^{1}H-NMR ($CDCl_3$; the integration values of 1/2 and 3/2 indicate protons of one of diastereomers; resonances not specified are of aromatic protons): δ 9.51 ((1/2)H, s), 9.45 ((1/2)H, s), 9.26 ((1/2)H, s), 9.20 ((1/2)H, s), 8.55 (1H, t, *J* = 5.0 Hz), 8.50 (1H, m), 8.23 (1H, m), 8.20 (1H, m), 7.9–7.85 (2H, m), 7.75–7.6 (6H, m), 7.55–7.4 (3H, m), 7.11 (2H, m), 7.05–6.85 (6H, m), 6.3–6.25 (2H, m), 6.07 (1H, m), 4.53 (1H, m, C*H*OH), 3.3–3.1 (2H, m, CH_2), 3.05–2.9 (2H, m, CH_2), 2.64 ((3/2)H, s, CH_3), 2.63 ((3/2)H, s, CH_3), 2.42 (3H, s, CH_3); ES–HRMS (CH_3CN): *m*/*z* calcd. for $C_{47}H_{40}IrON_6^+$ ([M–Cl]$^+$), 897.2887; found, 897.3015.

[Ir-L3]$^+$. ^{1}H-NMR ($CDCl_3$): δ 9.55 (1H, d, *J* = 8.7 Hz), 9.42 (1H, d, *J* = 8.2 Hz), 8.51 (1H, m), 8.22 (1H, d, *J* = 7.8 Hz), 8.2–8.1 (2H, m), 7.99 (1H, m), 7.82 (1H, d, *J* = 8.2 Hz), 7.75 (1H, d, *J* = 7.8 Hz), 7.65–7.55 (6H, m), 7.39 (1H, m), 7.3–7.2 (3H, overlapped with $CHCl_3$), 7.15 (1H, m), 7.0–6.85 (6H, m), 6.22 (1H, d, *J* = 7.3 Hz), 6.07 (1H, d, *J* = 6.9 Hz), 3.0–2.8 (4H, m, CH_2CH_2), 2.41 (3H, s, CH_3), 2.19 (3H, s, CH_3); ESI MS (CH_3CN): *m*/*z* calcd. for $C_{46}H_{38}IrN_6^+$ ([M–Cl]$^+$), 867.2782; found, 867.2809.

[Ir-L4]$^+$. ^{1}H-NMR ($CDCl_3$): *δ* 9.81 (1H, d, *J* = 8.2 Hz), 9.72 (1H, d, *J* = 8.2 Hz), 8.75–8.65 (2H, m), 8.5–8.35 (3H, m), 8.25 (1H, t, *J* = 7.4 Hz), 8.0–7.75 (8H, m), 7.72 (1H, d, *J* = 6.9 Hz), 7.75–7.65 (1H, m), 7.54 (1H, d, *J* = 5.5 Hz), 7.47 (1H, d, *J* = 6.4 Hz), 7.39 (1H, m), 7.34 (1H, dd, *J* = 6.8 Hz, 5.0 Hz), 7.1–6.9 (6H, m), 6.32 (1H, d, *J* = 6.9 Hz), 6.28 (1H, d, *J* = 6.8 Hz); ESI MS ([Ir-L4]$^+$, CH_3CN): *m*/*z* calcd. for $C_{44}H_{30}IrN_6^+$ ([M–PF_6]$^+$), 835.2156; found, 835.2249.

[Ir-X-Co] (X = L1, L2). Isolation of [Ir-X-Co] (= $[(\text{Ir-X})_n\text{Co}]^{(2+n)+}$, *n* = 1, 2 and 3) is exemplified by that of [Ir-L1-Co]. To a stirred solution of [Ir-L1]$^+$ (0.010 g, 2.2 mmol) in CH_3OH (10 mL), $CoCl_2 \cdot 6(H_2O)$ (0.89 mg, 0.75 mmol) was added at room temperature and the solution was stirred overnight. The volume of the solution was reduced and a saturated aqueous NH_4PF_6 solution was added, giving a yellow precipitate. The precipitate was filtered and washed with small amount of cold CH_3OH, followed by water and diethyl ether and dried in vacuum to give [Ir-L1-Co] as a yellow solid, 11 mg.

[Ir-L1-Co]. ESI–HRMS (CH_3CN): *m/z* calcd. for $C_{138}H_{114}N_{18}Ir_3Co^{5+}$ ($[M–5(PF_6)]^{5+}$, *n* = 3), 531.9536; found, 531.9650.

$[Ir\text{-}L2\text{-}Co]^{5+}$. ESI–HRMS ($CH_3CN$): *m/z* calcd. for $C_{141}H_{120}N_{18}O_3Ir_3Co^{5+}$ ($[M–5(PF_6)]^{5+}$, *n* = 3), 549.9599; found, 550.0667.

Hydrogen evolution experiment. Samples for photoinduced hydrogen production experiments were prepared in a 20-mL screw-cap glass vial with a silicone septum. Each sample was made in 10 mL H_2O/CH_3CN (1:1 v/v). Samples typically contained 15 μM $[Ir\text{-}X]^+$ or $[Ir(ppy)_2(bpy)]^+$, 5 μM $CoCl_2{\cdot}6(H_2O)$ or $[Co(bpy)_3]^{2+}$ and 0.015 or 1.2 M TEOA. The sample vial was capped and deoxygenated by bubbling Ar gas for 30 min. The vial was then placed over a magnetic stirrer in a dark place at room temperature and illuminated with visible light. Lax-Cute light source (100, xenon light) with complete heat blocking system from Asahi Spectra USA Inc. was used to illuminate only visible light (λ = 400–700 nm). After illumination, 1.0 mL of the gas produced in the vial was sampled using a Hamilton syringe. Gas chromatographic (GC) analysis for H_2 was performed on a Shimadzu GC-8A with a 5 Å molecular sieve column (3 m length), a rhenium-tungsten thermal conductivity detector, and Ar as a carrier gas. The calibration curve was created using Ar gas samples containing varying amounts of standard H_2 (99.9%, GL Sciences). Potassium ferrioxalate was used as a chemical actinometer to determine the photon flux at 411±5 nm (Asahi Spectra, MX0410),[7] which then was used for the determination of the quantum yield of H_2 generation.

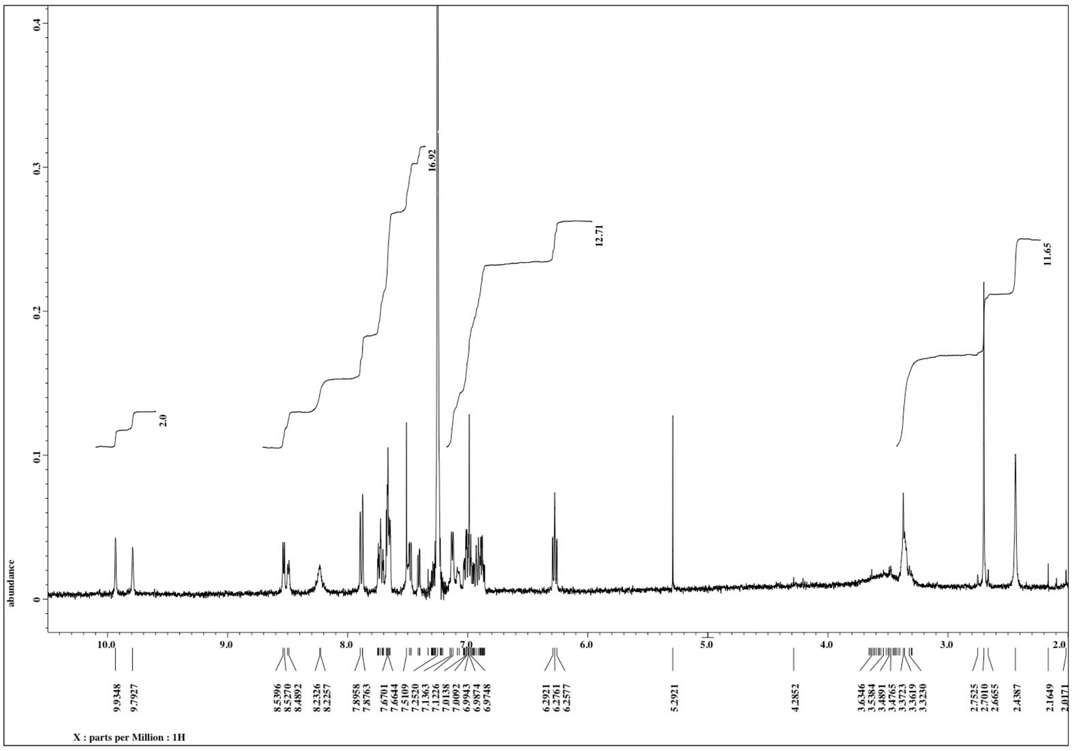
abundance
0
0.1
0.2
0.3
0.4
2.0
16.92
12.71
11.65
10.0
9.0
8.0
7.0
6.0
5.0
4.0
3.0
2.0
9.9348
9.7927
8.5396
8.5270
8.4892
8.2326
8.2257
7.8958
7.8763
7.6701
7.6644
7.5109
7.2520
7.1363
7.1226
7.0138
7.0092
6.9943
6.9874
6.9748
6.2921
6.2761
6.2577
5.2921
4.2852
3.6346
3.5384
3.4891
3.4765
3.3723
3.3619
3.3230
2.7525
2.7010
2.6665
2.4387
2.1649
2.0171
X : parts per Million : 1H

(a)

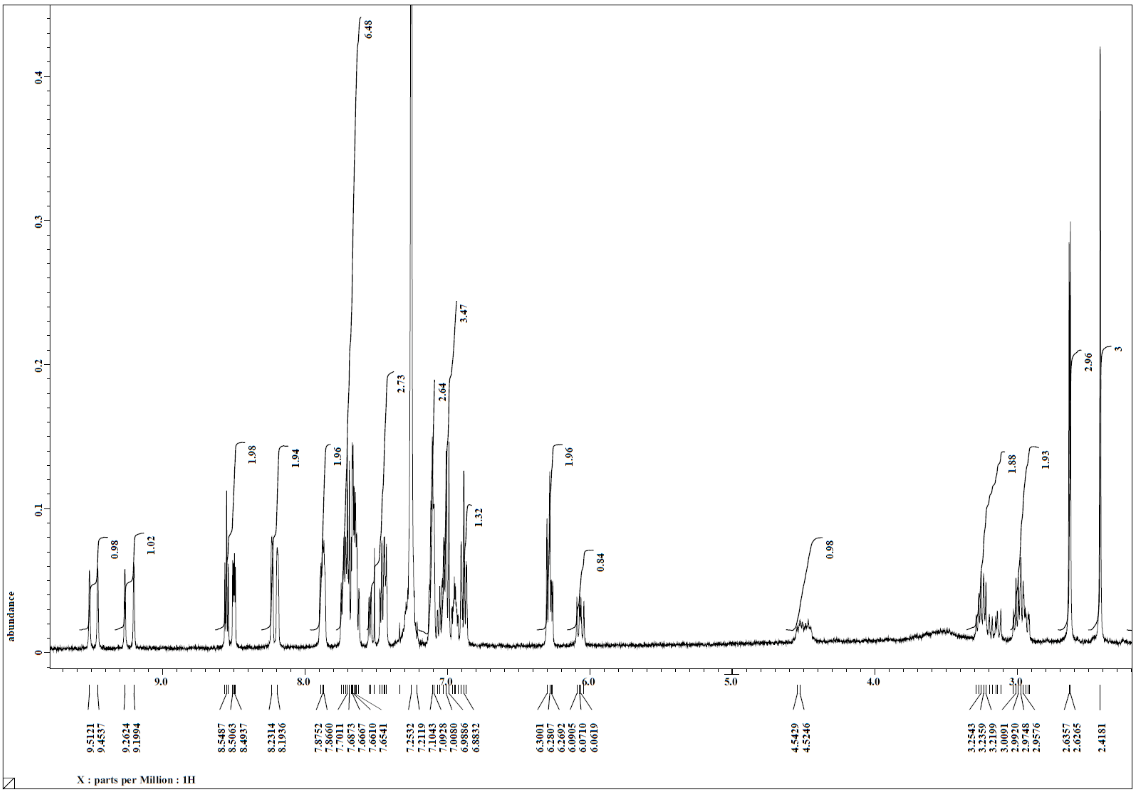
abundance
0
0.1
0.2
0.3
0.4
0.98
1.02
1.98
1.94
1.96
6.48
2.73
2.64
3.47
1.32
1.96
0.84
0.98
1.88
1.93
2.96
3
9.0
8.0
7.0
6.0
5.0
4.0
3.0
9.5121
9.4537
9.2624
9.1994
8.5487
8.5063
8.4937
8.2314
8.1936
7.8752
7.8660
7.7011
7.6873
7.6667
7.6610
7.6541
7.2532
7.2119
7.1043
7.0928
7.0080
6.9886
6.8832
6.3001
6.2807
6.2692
6.0905
6.0710
6.0619
4.5429
4.5246
3.2543
3.2359
3.2199
3.0091
2.9920
2.9748
2.9576
2.6357
2.6265
2.4181
X : parts per Million : 1H

(b)

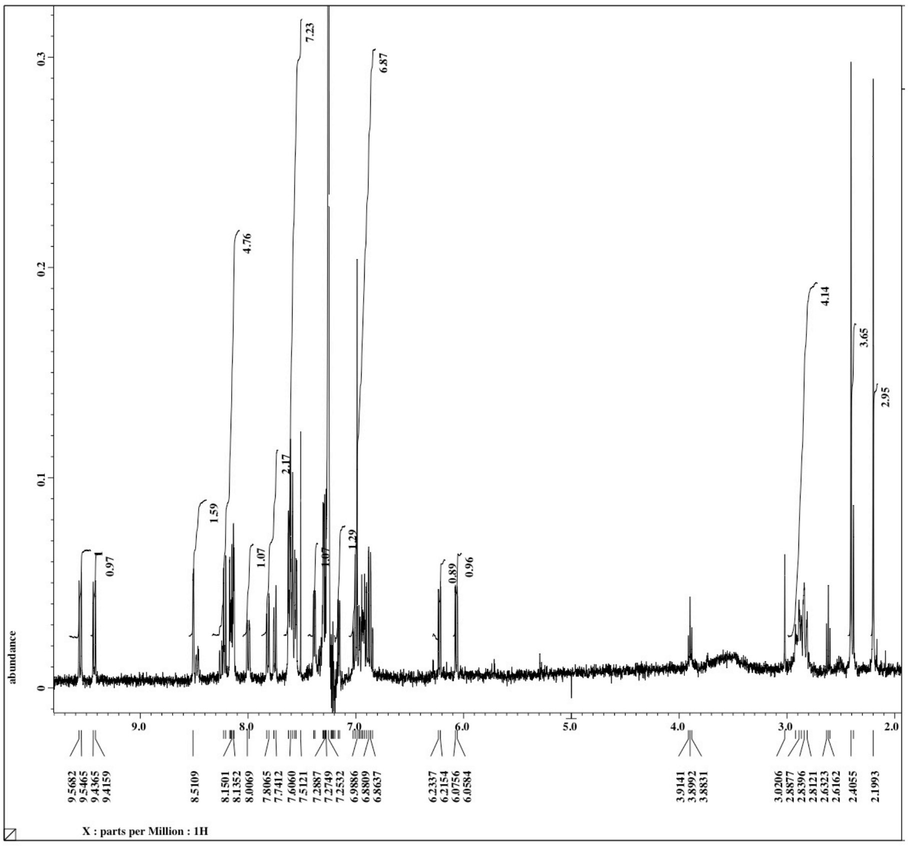

(c)

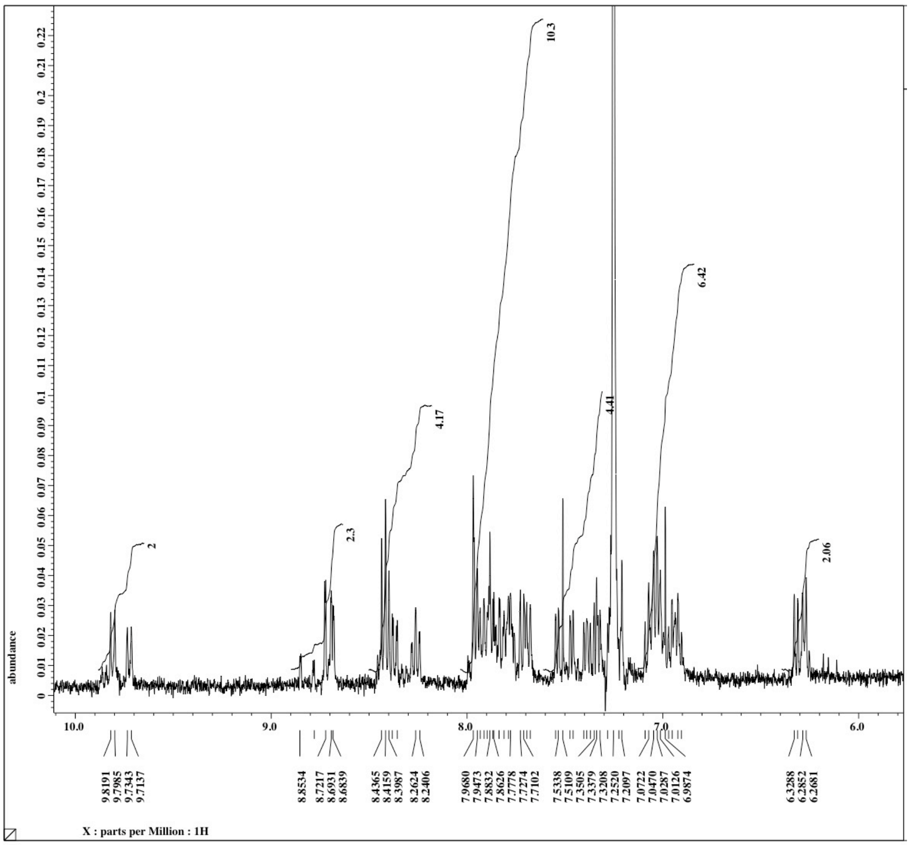

(d)

Fig. S1 ^{1}H-NMR spectra in $CDCl_3$. (a) $[Ir\text{-}L1]^+$. (b) $[Ir\text{-}L2]^+$. (c) $[Ir\text{-}L3]^+$. (d) $[Ir\text{-}L4]^+$.

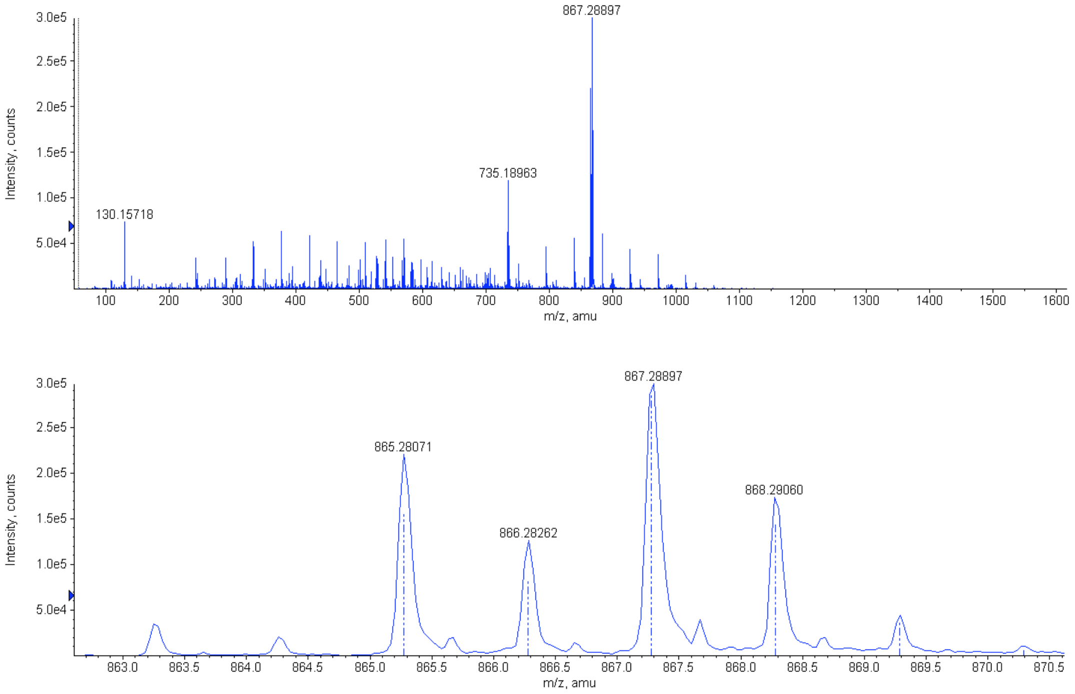
Intensity, counts
3.0e5
2.5e5
2.0e5
1.5e5
1.0e5
5.0e4
867.28897
735.18963
130.15718
100
200
300
400
500
600
700
800
900
1000
1100
1200
1300
1400
1500
1600
m/z, amu
Intensity, counts
3.0e5
2.5e5
2.0e5
1.5e5
1.0e5
5.0e4
867.28897
865.28071
868.29060
866.28262
863.0
863.5
864.0
864.5
865.0
865.5
866.0
866.5
867.0
867.5
868.0
868.5
869.0
869.5
870.0
870.5
m/z, amu

(a)

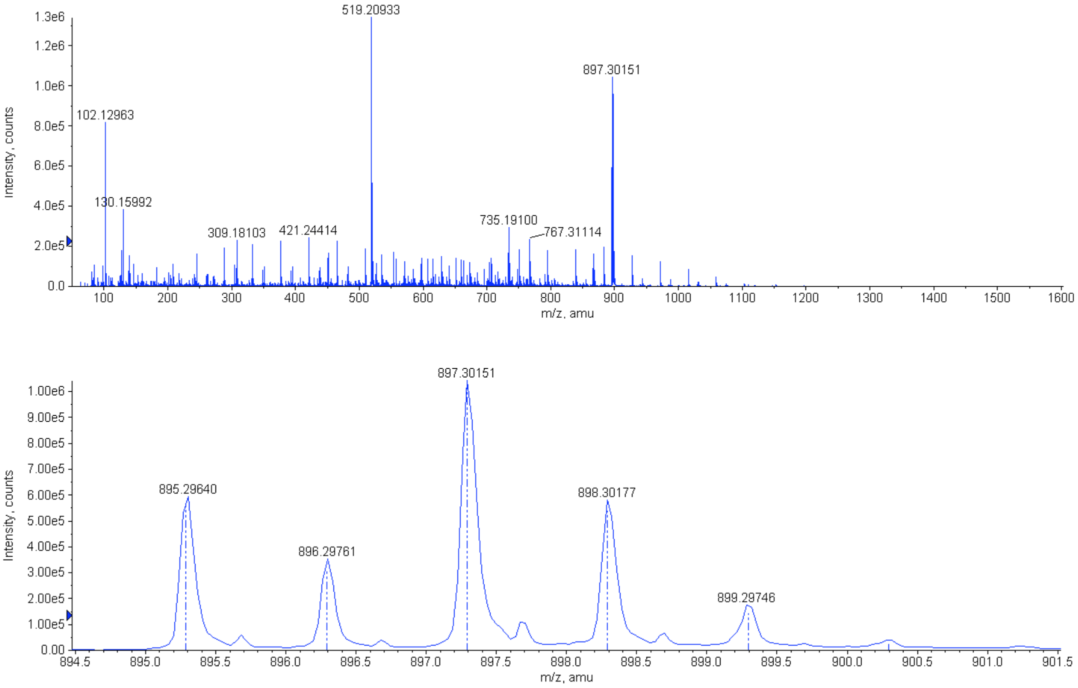
Intensity, counts
1.3e6
1.2e6
1.0e6
8.0e5
6.0e5
4.0e5
2.0e5
0.0
519.20933
897.30151
102.12963
130.15992
309.18103
421.24414
735.19100
767.31114
100
200
300
400
500
600
700
800
900
1000
1100
1200
1300
1400
1500
1600
m/z, amu
Intensity, counts
1.00e6
9.00e5
8.00e5
7.00e5
6.00e5
5.00e5
4.00e5
3.00e5
2.00e5
1.00e5
0.00
897.30151
895.29640
898.30177
896.29761
899.29746
894.5
895.0
895.5
896.0
896.5
897.0
897.5
898.0
898.5
899.0
899.5
900.0
900.5
901.0
901.5
m/z, amu

(b)

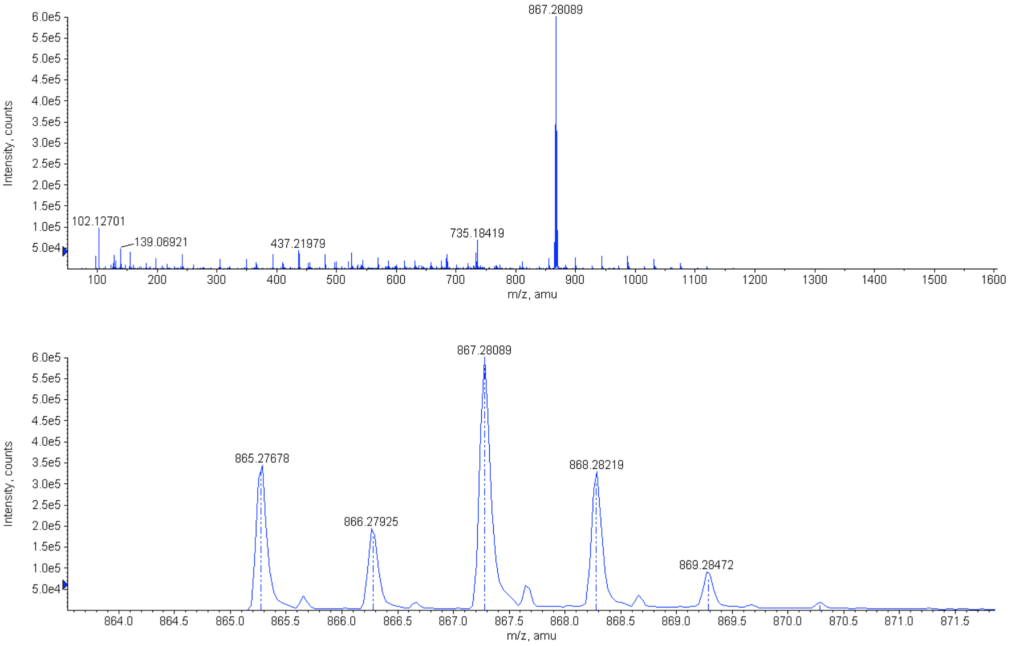

(c)

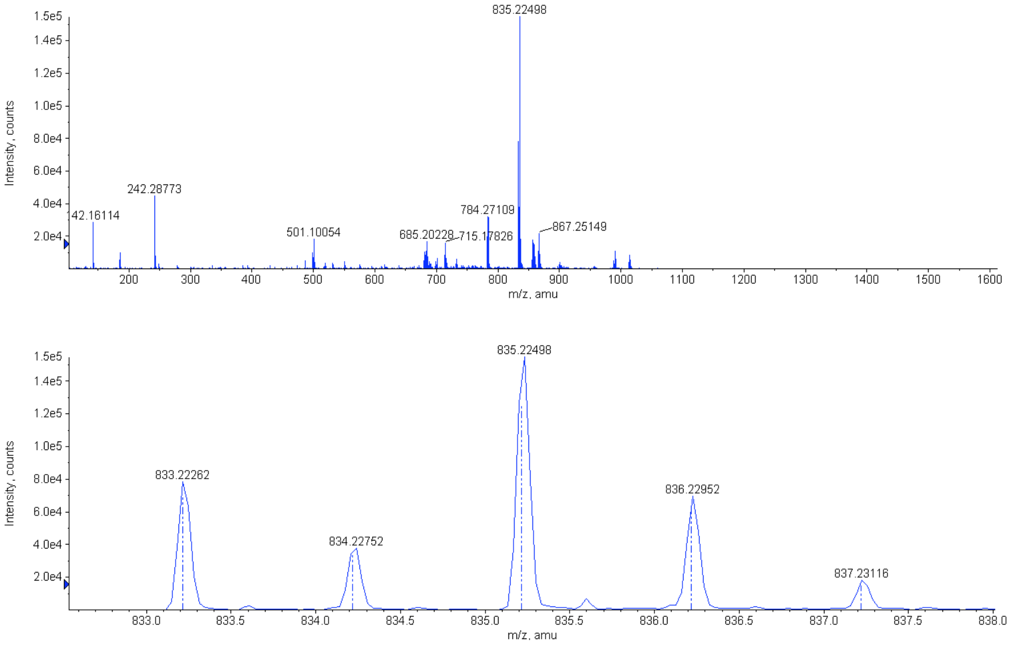

(d)

Fig. S2 ESI–HRMS spectra. CH_3CN was used as solvent. (a) [Ir-L1]$^+$. (b) [Ir-L2]$^+$. (c) [Ir-L3]$^+$. (d) [Ir-L4]$^+$.

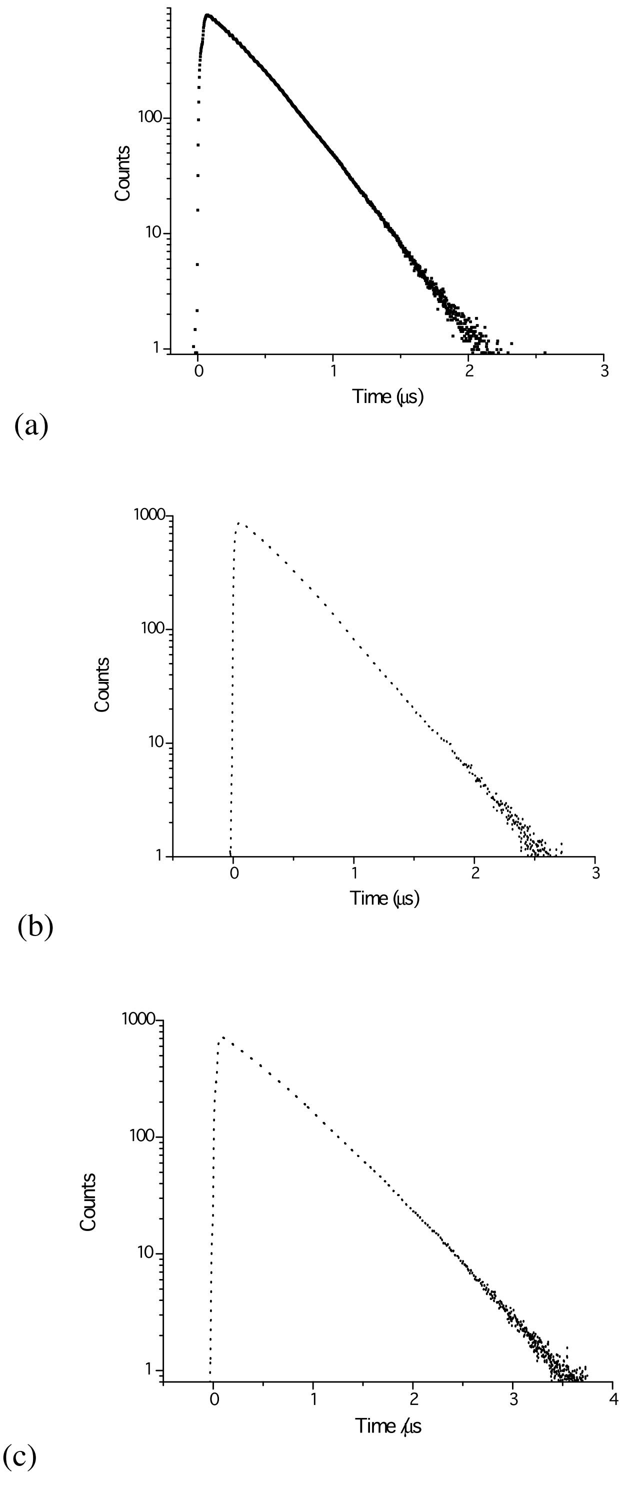

Fig. S3 Single exponential luminescence decay (logarithmic plot) for 6 μM $[Ir\text{-}X]^+$ in Ar degassed CH_3OH. (a) $[Ir\text{-}L1]^+$. (b) $[Ir\text{-}L2]^+$. (c) $[Ir\text{-}L3]^+$.

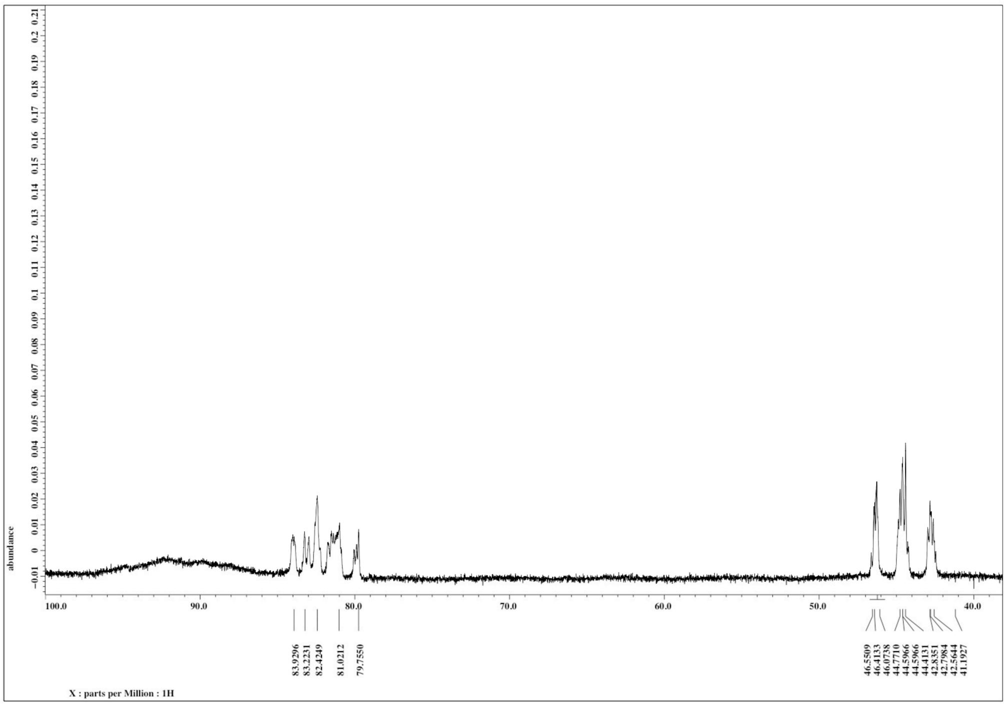

(a)

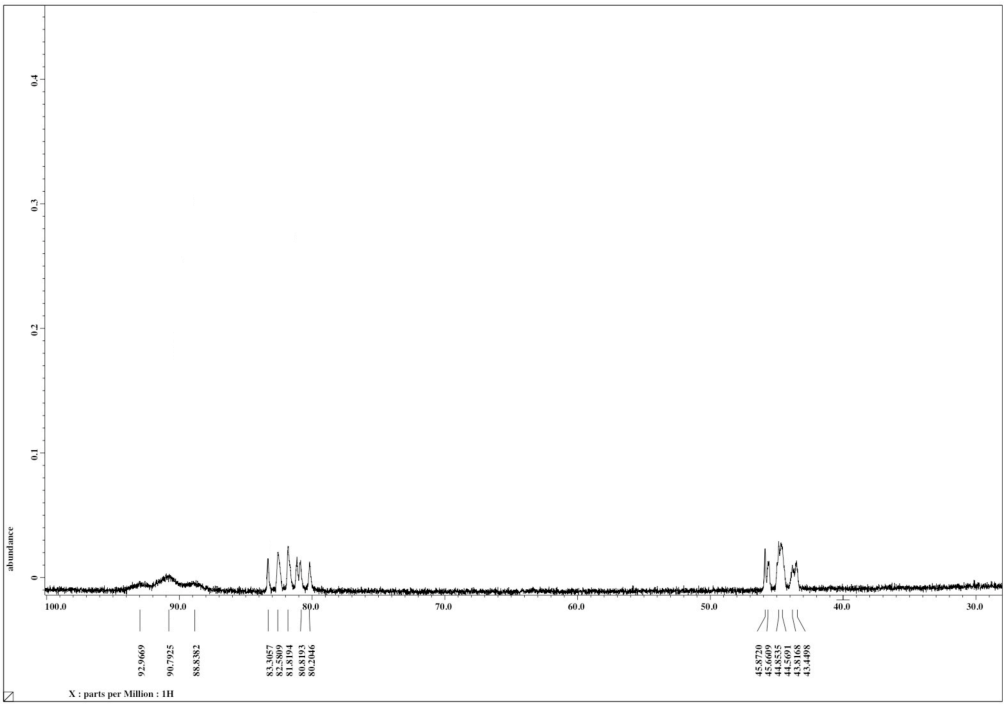

(b)

Fig. S4 ^{1}H-NMR spectra in CD_3CN for supramolecular complexes isolated as PF_6^- salt. (a) [Ir-L1-Co]. (b) [Ir-L2-Co].

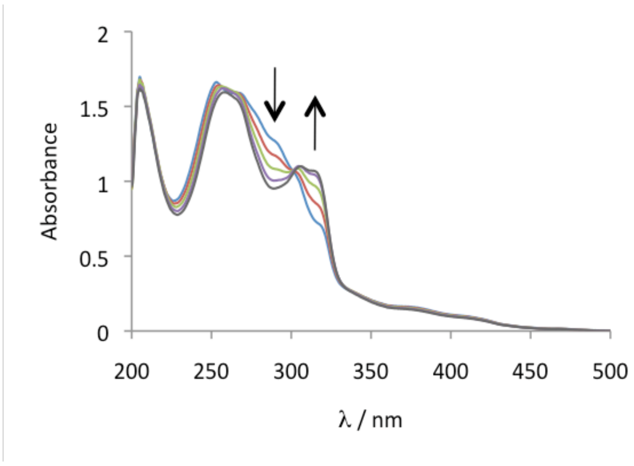

Fig. S5 Uv-visible absorption spectrophotometric titration spectra of $[Ir\text{-}L3]^+$ (30 µM) with $CoSO_4 \cdot 7(H_2O)$ (0–35 µM) in CH_3OH. Isosbestic point at 305 nm is observed, even though sequential binding of $[Ir\text{-}L3]^+$ and Co^{2+} is expected, which suggests the absorption spectra for $[(bpy)_nCo]^{2+}$ are similar around 305 nm, irrespective of *n*.

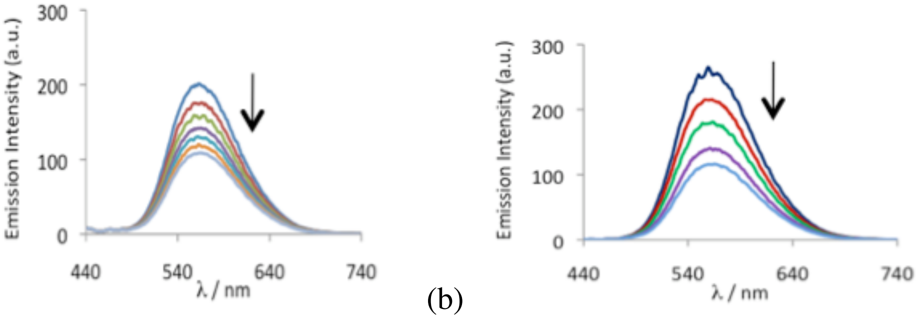

(a) (b)

Fig. S6 Emission quenching with $CoCl_2$ in Ar degassed H_2O/CH_3CN (1:1 v/v). λ_{ex} = 420 nm. (a) $[Ir\text{-}L1]^+$; 0–13.3 µM. (b) $[Ir\text{-}L2]^+$; 0–9.4 µM.

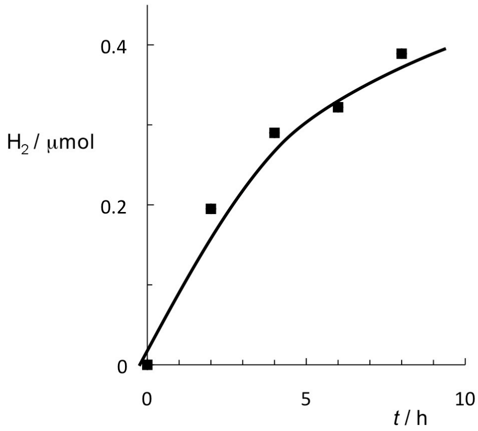

Fig. S7 Photochemical H_2 production from H_2O/CH_3CN (1:1 v/v) (10 mL) containing 15 mM TEOA, 15 μM $[Ir\text{-}L2]^+$ and 5 μM $CoCl_2$ at room temperature under Ar atmosphere.

Quantitative Estimation of Excited State Processes

The energy of the excited state. The energy of the excited state of $[\text{Ir-L1}]^+$ (E_{00}) is estimated using eq. S1:[8]

$$E_{00} = E_0 + (\text{FWHM})^2/(16\ k_B\ T \ln 2). \quad \text{(S1)}$$

Here, E_0 and FWHM are the energy of the emission maximum and the full width at half maximum in an energy scale, respectively, for the emission band, k_B is the Boltzmann constant and T the temperature. Putting in specific values, E_{00} is obtained as:

$$E_{00} = 2.21\ \text{eV} + (0.275\ \text{eV})^2/(16 \times 8.63 \times 10^{-5}\ \text{eV K}^{-1} \times 298\ \text{K} \times \ln 2)$$
$$= 2.48\ \text{eV}.$$

The driving force of the oxidative and reductive quenching. The oxidative quenching represented by reaction S2 and the reductive quenching by reaction S3 might be possible quenching mechanisms of $^*[\text{Ir-L1}]^+$ by electron transfer:

$$[^*\text{Ir}^{3+}\text{-L1-Co}^{2+}] \rightarrow [\text{Ir}^{4+}\text{-L1-Co}^{+}], \quad \text{(S2)}$$

$$\text{TEOA} + [^*\text{Ir}^{3+}\text{-L1-Co}^{2+}] \rightarrow \text{TEOA}_{ox} + [\text{Ir}^{2+}\text{-L1-Co}^{2+}]. \quad \text{(S3)}$$

The energetics for these processes are depicted in Fig. S8. The driving force for reaction S2, ΔG_{S2}, is, assuming a $[\text{Co(bpy)}_3]^{2+}$-type complex as the Co(II) species:

$$\Delta G_{S2} = e\ E([\text{Ir-L1}]^{2+/+}) - E_{00} - e\ E([\text{Co(bpy)}_3]^{2+/+})$$
$$= +0.89\ \text{eV} - 2.48\ \text{eV} - (-1.33\ \text{eV}) = -0.26\ \text{eV}.$$

The driving forces of reductive quenching by less coordinated Co(II) species, $[\text{Co(bpy)}_2]^{2+}$ and $[\text{Co(bpy)}]^{2+}$, would be progressively less exoergonic by ca. 0.15 V per one less bpy lignd.[9]

The driving force for the reductive quenching, reaction S3, ΔG_{S3}, is:

$$\Delta G_{S3} = -e\ E([\text{Ir-L1}]^{+/0}) - E_{00} + e\ E([\text{TEOA}_{ox}/\text{TEOA})$$
$$= -\ (-1.88\ \text{eV}) - 2.48\ \text{eV} + 0.33\ \text{eV} = -0.27\ \text{eV}.$$

Thus, both processes, eqs. S2 and S3, are energetically feasible.

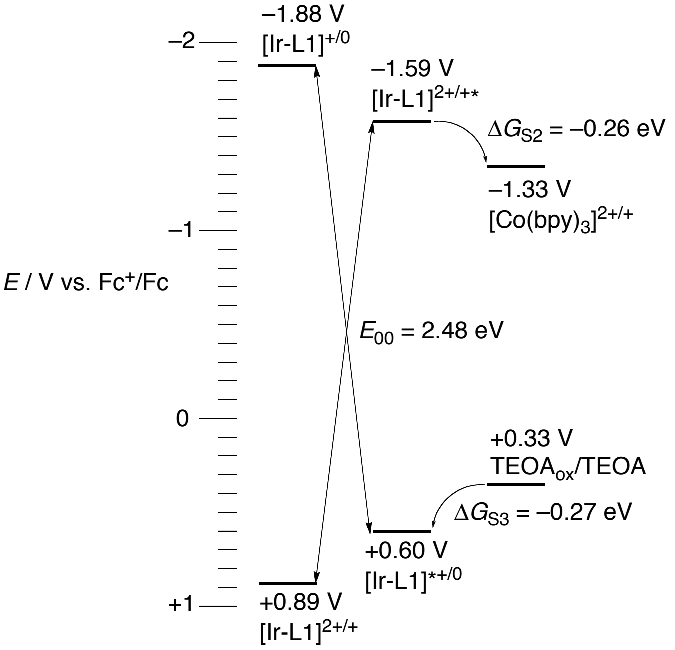

Fig. S8 Energetic relationship. Potentials are given in V with respect to Fc^+/Fc. The oxidation potential of TEOA is taken from the literature.[10] The value with respect to SCE has been converted to that with respect to Fc^+/Fc using the relationship, $E(Fc^+/Fc) = +0.40$ V vs. SCE.[11]

Excited Energy Transfer via the Förster Mechanism. Another process that has to be taken into account is intraensemble energy transfer, generically represented as eq. S4:

$$[{}^*Ir^{3+}\text{-}L1\text{-}Co^{2+}] \rightarrow [Ir^{3+}\text{-}L1\text{-}{}^*Co^{2+}]. \tag{S4}$$

The energy transfer via. the Förster mechanism is formulated as eq. S5:[12]

$$k_F = 8.80 \times 10^{-11} \frac{K^2 \phi_D}{n_S^{\;4}} \frac{(J_F/\mathrm{M^{-1}cm^{-1}nm^4})}{(\tau_D/\mathrm{s})(r/\mathrm{nm})^6} \mathrm{s^{-1}}. \tag{S5}$$

Here, ϕ_D and τ_D are the quantum yield of the emission and the excited state lifetime, respectively, of the donor in the absence of a quencher. K is an orientation factor, n_S is the refractive index of the solvent and r is the donor–acceptor separation. J_F represents the overlap of the donor emission and acceptor absorption and is defined as in eq. S6:

$$J_F = \frac{\int F_D(\lambda)\varepsilon_A(\lambda)\lambda^4 d\lambda}{\int F_D(\lambda) d\lambda}. \tag{S6}$$

Here, $F_D(\lambda)$ and ε_A are the emission spectrum of the donor and the molar absorption coefficient as functions of wavelength, λ.

We have assumed $K^2 = 2/3$, a value for random orientation, considering roughly spherical Ir(III) and Co(II) complexes and the flexibility of the linker unit, $-CH_2CH_2-$. The quantum yield is estimated as $\phi_D = 0.13$ on the basis of the relative luminescence intensity as compared to that of $[Ir(ppy)_2(bpy)]^+$ (0.06).[13] The refractive index of H_2O/CH_3CN is taken to be n_S = 1.34. The centre-to-centre distance may be around r = 0.8 nm, as the crystal structure of a dinuclear metal complex bearing the same bridging ligand shows,[14] although the distance may vary due to the flexibility of the linker unit. The excited state lifetime of $[Ir\text{-}L1]^+$ was experimentally obtained as $\tau_D = 353 \times 10^{-9}$ s (in CH_3OH). Although $[Co(bpy)_3]^{2+}$ is almost transparent in the visible region, weak d–d absorption bands ($\varepsilon \leq 50$ M^{-1} cm^{-1}) appear in a region that overlaps the luminescence of $[Ir\text{-}L1]^+$ (Fig. S9).[15] The value for J_F was obtained for $[Co(bpy)_3]^{2+}$ as 8.61×10^{11} M^{-1} cm^{-1} nm^4. Putting these values into eq. S4 gives the rate constant of the Förster energy transfer as $k_F = 2.2 \times 10^7$ s^{-1}. This value is larger than the decay rate constant ($\tau_D^{-1} = 2.8 \times 10^6$ s^{-1}) in the absence of quenching processes, which means that the energy transfer can be a quite efficient process following the excited state ([Ir*-L1-Co]) formation. Furthermore, once the cobalt(II) is reduced to cobalt(I), the visible absorption increases nearly three orders of magnitude, which should make the energy transfer process quite efficient.

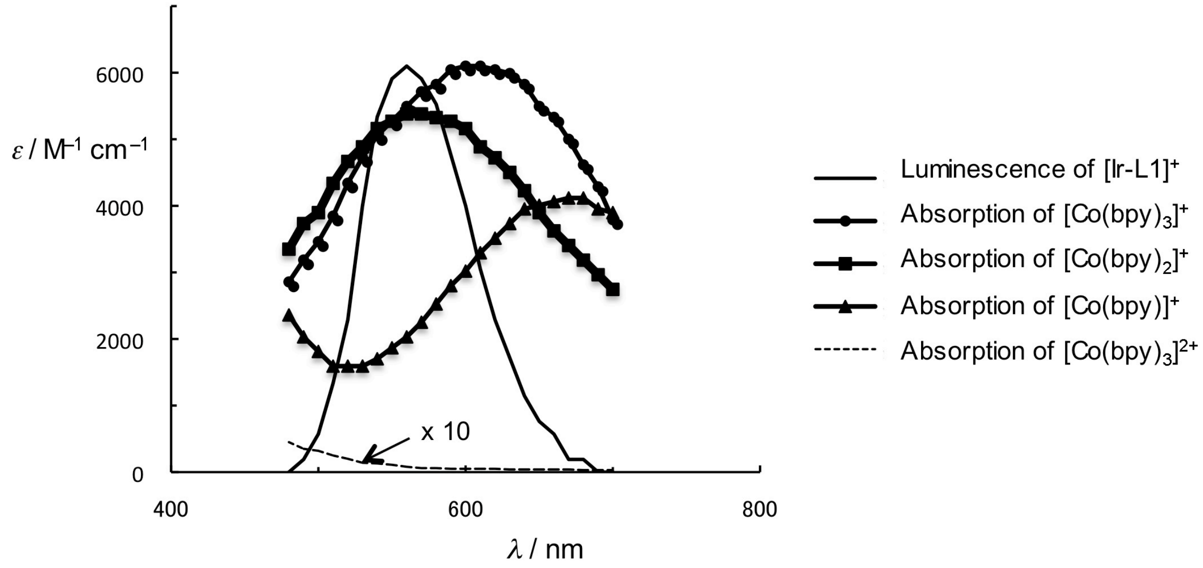

Fig. S9 Overlap of the luminescence from $*[Ir\text{-}L1]^+$ and the absorption of Co(II) species. The luminescence magnitude is arbitrary. Absorption data are taken from the literature.[9,15]

References

1. (a) S. Sprouse, K. A. King, P. J. Spellane and R. J. Watts, *J. Am. Chem. Soc.*, 1984, **106**, 6647–6653; (b) M. S. Lowry, W. R. Hudson, J. Robert A. Pascal and S. Bernhard, *J. Am. Chem. Soc.*, 2004, **126**, 14129–14135.

2. Y. Ohsawa, S. Sprouse, K. A. King, M. D. DeArmond, K. W. Hanck and R. J. Watts, *J. Phys. Chem.*, 1987, **91**, 1047–1054.
3. H. Nusbaumer, S. M. Zakeeruddin, J.-E. Moser and M. Grätzel, *Chem. Eur. J.*, 2003, **9**, 3756–3763.
4. (a) L. Sun, H. Berglund, R. Davydov, T. Norrby, L. Hammarström, P. Korall, A. Börje, C. Philouze, K. Berg, A. Tran, M. Andersson, G. Stenhagen, J. Mårtensson, M. Almgren, S. Styring and B. Åkermark, *J. Am. Chem. Soc.*, 1997, **119**, 6996–7004; (b) J.-C. Lepretre, B. Bar, J. Chauvin, A. Deronzier and B. Lefebvre, *Inorg. Chem. Commun.*, 2004, **7**, 47–50.
5. M. Furue, T. Yoshidzumi, S. Kinoshita, T. Kushida, S.-i. Nozakura and M. Kamachi, *Bull. Chem. Soc. Jpn.*, 1991, **64**, 1632–1640.
6. (a) Y.-Q. Fang and G. S. Hanan, 2003, 852–854; (b) R. Ziessel, J. Suffert and M.-T. Youinou, *J. Org. Chem.*, 1996, **61**, 6535–6546; (c) V. Grosshenny, F. M. Romero and R. Ziessel, *J. Org. Chem.*, 1997, **62**, 1491–1500.
7. C. G. Hatchard and C. A. Parker, *Proc. R. Soc. Lond. A*, 1956, **235**, 518–536.
8. K. A. Opperman, S. L. Mecklengurg and T. J. Meyer, *Inorg. Chem.*, 1994, **33**, 5295–5301.
9. H. A. Schwarz, C. Creutz and N. Sutin, *Inorg. Chem.*, 1985, **24**, 433–439.
10. K. Kasuga, H. Miyasaka, M. Handa and M. Dairaku, *Polyhedron*, 1995, **14**, 1675–1679.
11. N. G. Connelly and W. E. Geiger, *Chem. Rev.*, 1996, **96**, 877–910.
12. (a) J. Otsuki, *J. Porphyrins Phthalocyanines*, 2009, **13**, 1069–1081; (b) P. Klán and J. Wirz, *Photochemistry of Organic Compounds*, Wiley, West Sussex, 2009; (c) S. E. Braslavsky, E. Fron, H. B. Rodríguez, E. S. Román, G. D. Scholes, G. Schweitzer, B. Valeur and J. Wirz, *Photochem. Photobiol. Sci.*, 2008, **7**, 1444–1448.
13. J. I. Kim, I.-S. Shin, H. Kim and J.-K. Lee, *J. Am. Chem. Soc.*, 2005, **127**, 1614–1615.
14. S. Ferrerei and C. M. Elliott, *Inorg. Chem.*, 1995, **34**, 5818–5824.
15. Y. Sasaki, *Bull. Inst. Chem. Res. Kyoto Univ.*, 1980, **58**, 187–192.